ACS Catalysis

Research Article

pubs.acs.org/acscatalysis

Role of Dissociation of Phenol in Its Selective Hydrogenation on Pt(111) and Pd(111)

Gaofeng Li,[†,‡] Jinyu Han,[†] Hua Wang,[†] Xinli Zhu,*[,†] and Qingfeng Ge*[,†,‡]

[†]Collaborative Innovation Center of Chemical Science and Engineering, School of Chemical Engineering and Technology, Tianjin University, Tianjin 300072, China

[‡]Department of Chemistry and Biochemistry, Southern Illinois University, Carbondale, Illinois 62901, United States

Supporting Information

ABSTRACT: The adsorption, dissociation, and hydrogenation of phenol on the Pt(111) and Pd(111) surfaces have been studied using density functional theory slab calculations. The results show that phenol favors adsorption through a mixed $\sigma-\pi$ interaction on both surfaces through its phenyl ring, with the hydrogen atoms and hydroxyl tilted away from the surface. The dissociation of phenol to phenoxy is both thermodynamically and kinetically favored on Pd but not on Pt. The phenoxy adsorbs on Pd through both the phenyl ring and the oxygen atom, whereas the O atom points away from the surface on Pt. On Pt, the barrier for adding one hydrogen atom to the adsorbed phenol is 0.49 eV lower than the overall barrier for phenol dissociation to phenoxy followed by adding the hydrogen atom to its phenyl ring, resulting in direct hydrogenation of the adsorbed phenol to cyclohexanol as the dominant reaction pathway. In contrast, on Pd, the barrier for direct hydrogenation (1.22 eV) is higher than the overall barrier of dissociation followed by the hydrogenation process (0.85 eV), resulting in hydrogenation of the adsorbed phenoxy to cyclohexanone as the major reaction pathway. Microkinetics analysis confirms that hydrogenation of the adsorbed phenol is the dominant pathway on Pt, whereas phenoxy hydrogenation drives the turnover on Pd. These results are consistent with the experimentally observed selectivity of phenol hydrogenation on Pd and Pt catalysts.

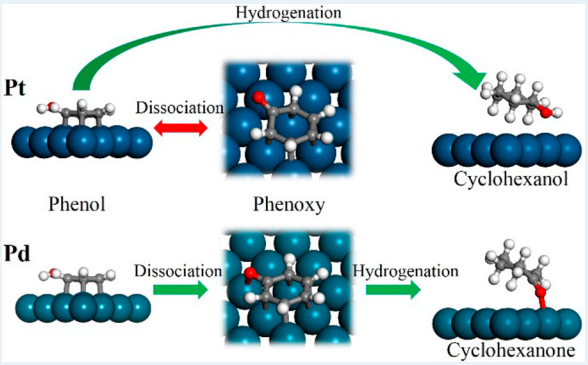

KEYWORDS: *phenol, cyclohexanol, cyclohexanone, Pt, Pd, selective hydrogenation, DFT*

1. INTRODUCTION

Catalytic conversion of biomass to fuels and chemicals is of importance for sustainability in the future. As a major fraction of biomass, lignin can be depolymerized to phenolics,[1−8] which is a good source for production of chemicals and fuels through hydrogenation and hydrodeoxygenation reactions. Phenol has the simplest representative structure of phenolic compounds, and thus, it has been widely used as a model compound for hydrogenation and hydrodeoxygenation to produce fuels and chemicals.[9−12]

Low-temperature hydrogenation of phenol is an industrial reaction to produce cyclohexanol and cyclohexanone, which are starting compounds to manufacture various industrially important chemicals. This hydrogenation can be realized in both liquid and vapor phases at relatively low temperatures (30−250 °C), with or without added pressure. Many supported metal catalysts have been tested to control the selectivities of cyclohexanol and cyclohexanone.[13−19] Talukdar et al.[15] studied hydrogenation of phenol on supported Pt and Pd catalysts at 523 K and 1 MPa. These authors reported that cyclohexanol was the major product on Pt catalysts, with cyclohexanol and cyclohexanone selectivities of 90% and 8%, respectively, on Pt/alumina. On supported Pd catalysts, cyclohexanone became the major product, with cyclohexanol and cyclohexanone selectivities of 11% and 88%, respectively. Lately, a number of works reported that supported Pd catalysts were selective to produce cyclohexanone, and the selectivity could be further improved by modifying the support properties,[20−26] such as adding Lewis acid.[25,27]

Though the detailed reaction mechanism is not clear yet, it is generally believed that phenol is first hydrogenated to cyclohexenol, which then tautomerizes to cyclohexanone quickly, and cyclohexanone may be further hydrogenated to cyclohexanol.[25,28,29] However, several recent theoretical studies raised doubts about this mechanism when the hydrogenation reaction was carried out in the absence of water. It has been shown that the activation barrier for tautomerization from cyclohexenol to cyclohexanone is 221 kJ/mol in the absence of water, which is considered too high to take place under the reaction conditions.[22] Yoon et al. found that the activation barriers for tautomerization from 1,3-cyclohexadienol to 3-cyclohexenone on the Pt(111) and Ni(111) surfaces were 184 and 106 kJ/mol, respectively. These barriers are higher than that for further hydrogenating 1,3-cyclohexadienol in vapor

Received: November 13, 2014
Revised: January 22, 2015
Published: February 17, 2015

DOI: 10.1021/cs501805y
ACS Catal. 2015, 5, 2009−2016

phase.[12] The authors therefore concluded that phenol can be hydrogenated all the way to cyclohexanol over the Pt and Ni catalysts without the tautomerization step in a vapor phase reaction. However, in the presence of water, the activation barrier for tautomerization is significantly lowered due to the participation of proton, resulting in tautomerization as the preferred route in an aqueous phase hydrogenation. We note that the surface dissociation of phenol into phenoxy has not been considered in those studies. However, the dissociation of phenol to phenoxy was found to readily occur and has been observed at 200 K on Pt(111) in temperature-programmed desorption of phenol.[30] Computational study showed that the dissociation process by breaking the O−H bond is preferred on the Rh(111) surface over the Pt(111) surface.[31] Therefore, the phenoxy species should be present on the surface, which may compete with adsorbed phenol as the initial species for hydrogenation and result in different products.

In this contribution, the adsorption, dissociation, and hydrogenation of phenol on the Pt(111) and Pd(111) surfaces were studied using density functional theory (DFT) slab calculations. The results showed that the thermodynamic and kinetic favorability of phenol dissociation to phenoxy determines the major surface species being hydrogenated, and further influences the final product selectivity. A microkinetics analysis was performed on the basis of the adsorption energies, activation barriers, and preexponential factors from DFT calculations. The findings in this work not only shed light on the observed selectivity of phenol hydrogenation but also are of importance in understanding and optimizing the hydrogenation and hydrodeoxygenation of phenolic compounds over the supported metal catalysts.

2. COMPUTATIONAL METHOD

All calculations were performed using the Vienna Ab Initio Simulation Package (VASP).[32,33] Projector augmented wave (PAW) potentials[34,35] were used to represent the effective cores. Electronic optimization was performed self-consistently using the plane wave basis set with a cutoff energy of 400 eV. The Perdew−Burke−Ernzerhof (PBE) functional[36] was used to describe exchange and correlation effects. The atomic structures were relaxed using either the quasi-Newton scheme or conjugate gradient algorithm as implemented in the VASP code. To examine the effect of van der Waals (vdW) interaction on adsorption energies and activation barriers, we used the optB88-vdW[37] functional with the PBE−PAW potential in several selected adsorption configurations and elementary steps.

The Pt(111) and Pd(111) surfaces were modeled with p (4 × 4) surface unit cells and four layered slabs separated by at least 15 Å of vacuum. The atoms in the bottom two layers were fixed at the corresponding bulk positions, and those in the top two layers together with the adsorbate atoms were allowed to relax. Computed bulk lattice constants of 3.978 and 3.955 Å for Pt and Pd, respectively, were used to construct the slabs. For geometry optimization, a (2 × 2 × 1) grid was used to generate the k-points. Test calculations using a (4 × 4 × 1) k-point grid showed that the adsorption energy of phenol is converged to <0.1 eV and activation barrier is converged to ∼0.01 eV.

To calculate the adsorption energy, the following equation was used:[38]

$$E_{ads} = E_{(adsorbate/suface)} - E_{(adsorbate)} - E_{(bare\ surface)} \quad (1)$$

where $E_{(molecule/surface)}$ is the total energy of an adsorbate bound to the metal slab, $E_{(adsorbate)}$ is the total energy of a molecule in gas phase or an isolated intermediate, $E_{(bare\ surface)}$ is the total energy of the bare slab. Positive values of the adsorption energy indicate that the adsorption is endothermic, whereas the negative values correspond to exothermic adsorption. Stationary and transition states were confirmed by a normal-mode analysis; no imaginary mode was found for optimized stable structures, and only one imaginary mode was found for the transition states.

3. RESULTS AND DISCUSSION

3.1. Phenol Adsorption on Pt(111) and Pd(111).

Several initial configurations of phenol adsorption on the Pt(111) and Pd(111) surfaces were constructed and optimized. Geometry optimization results showed the upright adsorption of phenol through O interacting with the surface atoms was unstable, whereas several adsorption configurations through C interacting with the surface atoms were stable. These stable configurations include adsorption on the bridge and hollow sites with the phenyl ring almost in parallel with the surfaces, as well as the bent adsorption through a carbon atom binding a single metal site. The optimized stable configurations were provided in Figure S1 with the corresponding adsorption energies. Among these configurations, Bri 30, which is shown in Figure 1, is the most stable one on both Pt (111) and Pd(111) and was used as the initial structure for the subsequent dissociation and hydrogenation studies. As shown in Figure 1, C_2 and C_5 are σ-bonded to the corresponding surface metal atoms, where C_1 and C_6 as well as C_3 and C_4 share a surface metal atom in a π-bond mode. On Pt(111), the bond length of Pt−C_1 is 2.30 Å, and the other Pt−C bond lengths are 2.16−2.20 Å, in good agreement with previous results.[12,31] On Pd(111), the bond length of Pd−C_1 is 2.32 Å, and the lengths of other Pd−C bonds are 2.19−2.23 Å. The slightly longer bond length suggests weaker adsorption of phenol on Pd than

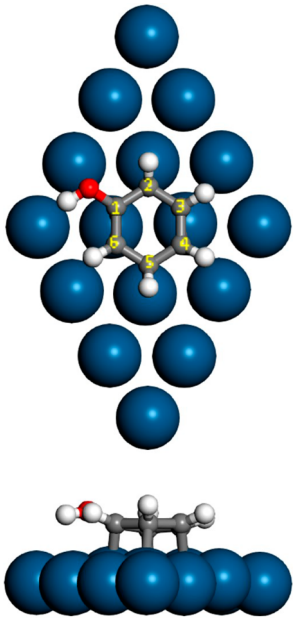

Figure 1. Schematic top view (upper) and side view (lower) of phenol adsorption on Pt (111) and Pd (111) in the Bri 30 configuration. Carbon atoms of phenol were labeled with number clockwise. The Pt and Pd atoms are in blue and the O, H, and C atoms are in red, white, and gray, respectively.

DOI: 10.1021/cs501805y
ACS Catal. 2015, 5, 2009−2016

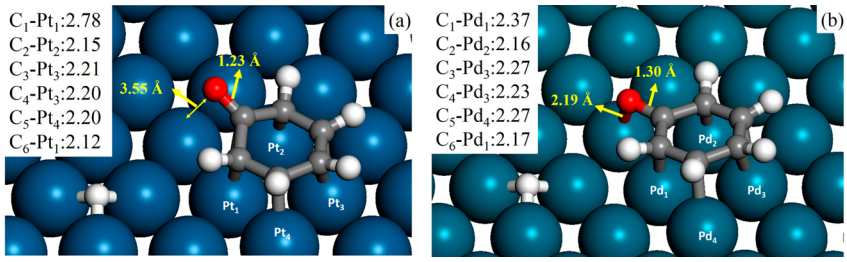

Figure 2. Coadsorbed phenoxy and H adatom on (a) Pt(111), and (b) Pd(111) as products of phenol dissociation. The Pt and Pd atoms are in blue, and the O, H, and C atoms are in red, white, and gray, respectively. Distances are in Å.

on Pt. On both surfaces, the OH group tilts away from the surface. The angle between the OH group and the surface plane are 42.4°and 20.1° for Pt and Pd, with the lengths of C−O bond being 1.36 and 1.37 Å, respectively. The distances between oxygen and the nearest Pt and Pd atoms are 3.08 and 2.94 Å, respectively. We note that all H atoms in C−H bonds tilt away from the surfaces.

The adsorption energies of phenol on Pt(111) and Pd(111) in the Bri 30 configuration are −1.16 eV and −1.04 eV, respectively. The adsorption energy on Pd(111) is consistent with the reported value of −1.39 eV,[39] which was calculated using DMol3 of Materials Studio on a three-layer Pd slab in a (3 × 3) surface unit cell. We also used the optB88-vdW functional and tested the effect of including vdW correction. The adsorption energy on Pt(111) by taking vdW interactions into account is −2.06 eV, higher than the value of −1.78 eV in c(2 × 4) supercell slab models (16 surface atoms)[12] but lower than the value of −2.23 eV in 4 × 6 atoms per surface unit cell and slab layer.[31] The differences may originate from the different symmetry and sizes of the surface unit cell and thereby different surface phenol coverages used in those calculations. It has been reported that the overall potential energy trend calculated using the vdW functionals, including activation energy, are qualitatively similar to that calculated from the PBE functional.[40] Therefore, we report the results based on the pure PBE functional in the present study.

3.2. Phenol Dissociation on Pt(111) and Pd(111). Dissociative adsorption of phenol by breaking the O−H bond leads to coadsorbed phenoxy and H adatom. The optimized coadsorption structures of phenoxy and H atom on Pt(111) and Pd(111) are shown in Figure 2. Compared to the adsorbed phenol, the Pt−C_1 distance of surface phenoxy increases significantly to 2.78 Å, whereas other Pt−C distances only slightly change to 2.12−2.20 Å. Moreover, the distance between O and the nearest surface Pt increases substantially from 3.08 to 3.55 Å. These changes indicate that both O and C_1 are repelled from the surface as a result of breaking the O−H bond. The increased distance from C_1 and O to the surface weakens the adsorption of phenoxy on Pt(111). The adsorption structure of phenoxy on Pt(111) is similar to the η^5-π-adsorption mode on Pt surface proposed on the basis of an experimental study.[30] In contrast to phenoxy on Pt, the Pd−C_1 distance is only slightly elongated to 2.37 Å, with other Pd−C distances slightly changed to 2.16−2.27 Å. The most significant change from that of phenol adsorption structure is the distance between O and the nearest Pd, which is reduced from 2.94 to 2.19 Å. At this distance, a Pd−O bond is formed. To confirm the formation of the Pd−O bond, we performed an analysis of the projected density of states of Pd and O for the adsorbed phenoxy on Pd(111) and plotted the results in Figure 3. As

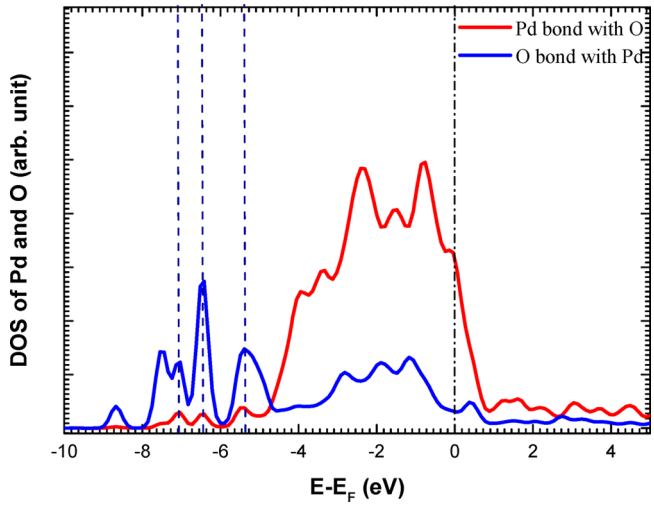

Figure 3. Projected density of states (DOSs) of O atom (blue line) and the Pd atom (red line) directly involved in bonding with O. The dotted dash line indicates Fermi level; the dashed lines indicate direct overlap between O and Pd.

shown in Figure 3, there are significant overlaps between the d states of Pd and the p orbitals of O, strongly indicating bonding interaction between O and Pd. The formation of the Pd−O bond will strengthen the interaction of phenoxy with the Pd surface as compared with phenol. Indeed, the calculated coadsorption energies of phenoxy and H adatom (the H adatom occupying the adjacent hollow site) on Pt and Pd are −0.88 eV and −1.08 eV, respectively. Interestingly, the relative stability of phenoxy on Pt and Pd is a reverse of that of phenol on the two surfaces. On the basis of the calculated adsorption energies, we determined the reaction energies of phenol dissociation on Pt and Pd are 0.28 eV and −0.03 eV, respectively. These results indicate that the dissociation is exothermic on Pd but endothermic on Pt. Taking into account zero-point energy and entropy contributions, we calculated the Gibbs free energy change for phenol dissociation to be −0.08 eV on Pd and 0.27 eV on Pt at 423 K. These results indicate that the formation of phenoxy is thermodynamically favorable on Pd but not on Pt.

To explore the kinetic aspect of phenol dissociation, we calculated the activation barriers. As shown in Figure 4, the dissociation barrier of phenol is 0.48 eV on Pt and 0.20 eV on Pd. These results indicate that phenol dissociation on Pd is kinetically more favorable than on Pt. On the other hand, both activation barriers are low, and therefore, dissociation can occur at relatively low temperatures on both surfaces. These results also show that the dissociation and its reverse reaction (i.e., the recombination of phenoxy and H adatom) are reversible

DOI: 10.1021/cs501805y
ACS Catal. 2015, 5, 2009−2016

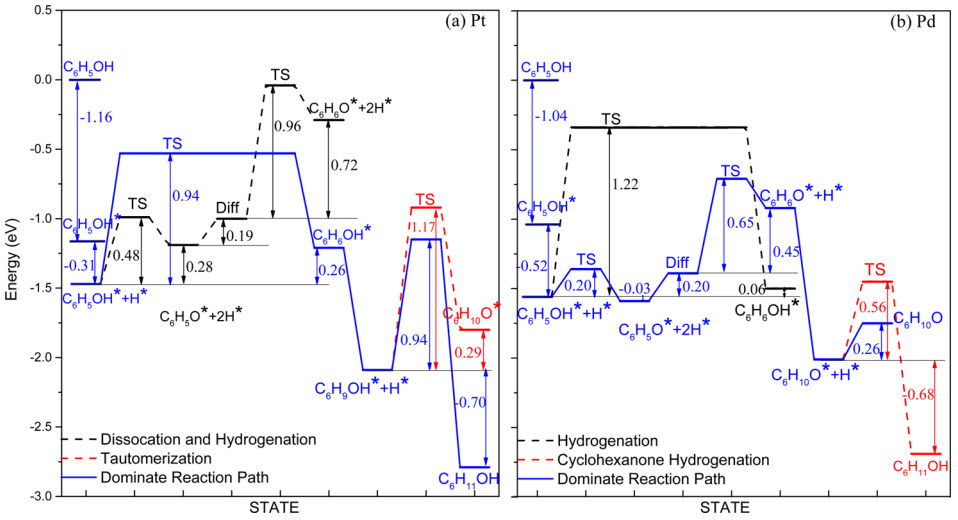

Figure 4. Potential energy profiles of phenol hydrogenation on (a) Pt and (b) Pd. Blue solid line indicates major reaction pathway, and dashed black and red lines are alternative pathways. A* represents the adsorption state of species A on the surface. "Diff" is short for diffusion. The diffusion is the step that hydrogen atom away from the reaction site move to the reaction site.

Scheme 1. Major Reaction Pathway of Phenol Hydrogenation on Pt (Upper) and Pd (Lower)[a]

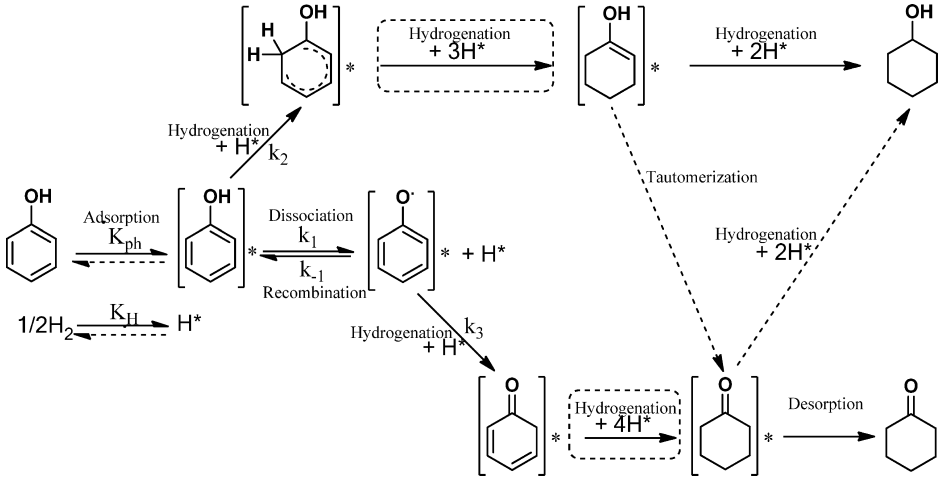

[a]The * represents surface adsorption site. Solid line step, major reaction path; dashed line step, minor reaction path; steps in dashed line box were not studied in detail in this work.

reactions.[31] The activation barrier for the reverse reaction is 0.20 eV on Pt, significantly lower than the forward reaction barrier (0.48 eV). Combining with the relative thermodynamic stability of adsorbed phenol and coadsorbed phenoxy and H adatom, we predict that phenol is the dominant species on Pt. In contrast, the activation barrier for phenoxy and H adatom recombination on Pd is only 0.23 eV, slightly higher than that of dissociation reaction. Again, considering the relative stability, we anticipate that the surface phenoxy species is an important intermediate and will be available for further hydrogenation on Pd.

We tested the effect of coadsorbed hydrogen on the dissociation barrier by adding up to three H atoms to the hollow sites in the unit cell. Compared to the results on the surface without coadsorbed H adatoms, the presence of the H adatoms did not change the structures of adsorbed phenol, transition states of phenol dissociation, and the final coadsorbed phenoxy and H adatom. Furthermore, the activation barrier only changed by ~0.01 eV, and the overall reaction energy changed by ~0.03 eV in the presence of H adatoms. These results strongly indicate coadsorbed H adatom has negligible effect on phenol dissociation as long as the neighboring hollow site is available. Our kinetics analysis showed that the surface is predominantly occupied by phenol. The surface coverage of hydrogen is low.

3.3. Hydrogenation of Phenol and Phenoxy on Pt(111) and Pd(111). After establishing the stable configurations of adsorbed phenol and phenoxy, we then investigated hydrogenation of the phenyl ring. The major reaction steps are shown in Scheme 1. Comparing the energies after the first hydrogen was added to different carbon atoms of the phenyl ring on Pt(111), it is not surprising that the intermediate formed from hydrogenating C_1 has the highest energy of −1.07 eV. After C_1 is hydrogenated, the Pt−C_1 bond becomes significantly longer than the other Pt−C bonds. Five other intermediates from hydrogenating the C_{2-6} atoms have adsorption energies in the range between −1.20 and −1.32 eV, with the intermediate formed from adding hydrogen to C_6 having the lowest energy (−1.32 eV). This result suggests that thermodynamically the C_{2-6} carbons have a similar possibility

DOI: 10.1021/cs501805y
ACS Catal. 2015, 5, 2009−2016

to be hydrogenated and C_1 should be the last carbon to be hydrogenated. The activation barrier for adding the first hydrogen to C_6 of adsorbed phenol was then calculated and compared to that for phenol dissociation to coadsorbed phenoxy and H adatom and then adding the hydrogen atom to C_6 of phenoxy (Scheme 1 and Figure 4A). Obviously, phenol dissociation followed by hydrogenation path is strongly endothermic. This pathway has an overall barrier of 1.43 eV, which is 0.49 eV higher than that for directly hydrogenating phenol (0.94 eV). These results indicate that direct hydrogenation for phenol on Pt(111) is both thermodynamically and kinetically a favored pathway and is expected as a key step for low temperature hydrogenation of phenol. Under this condition, the surface phenoxy species acts as a spectator during the reaction. On the other hand, the difference between the two barriers can be overcome if reactions occur at high temperatures, enabling hydrogenation of the phenoxy species. Indeed, Nie and Resasco recently proposed that the tautomerization of m-cresol (3-methylphenol) to 3-methyl-3,5-cyclohexadienone is the first step for m-cresol hydrodeoxygenation,[41] which could be considered as cresol dissociation to phenoxy followed by phenoxy hydrogenation.

The adsorption energies of the intermediates formed from adding hydrogen atoms to the phenyl ring consecutively were also calculated, and the results do not show specific thermodynamic preferences. Yoon et al.[12] suggested that adding the first hydrogen atom to the phenyl ring has the highest reaction barrier for phenol hydrogenation on Ni(111) and Pt(111). Consequently, the subsequent hydrogenation could occur spontaneously and randomly once the first hydrogen was added. One question remains to be answered: is phenol hydrogenated all the way to cyclohexanol directly or is phenol hydrogenated to cyclohexenol first and then tautomerized to cyclohexanone followed by further hydrogenation to cyclohexanol (Scheme 1)? To explore whether tautomerization was involved in the reaction or not, the activation barriers for tautomerization from cyclohexenol to cyclohexanone and hydrogenation of cyclohexenol to cyclohexanol were computed. These barriers were included in Figure 4a for comparison. The activation barrier of a surface-mediated tautomerization pathway (1.17 eV) is higher than that of the direct hydrogenation pathway (0.94 eV) on Pt, predicting that the direct hydrogenation pathway will be the dominating reaction route under typical phenol hydrogenation conditions. It is worth noting that the tautomerization process of enol to ketone in this calculation is a surface-assisted process (i.e., H transfers through the metal surface). This process has an activation barrier significantly lower than 2.29 eV of intramolecular tautomerization, i.e. hydrogen transfer without the assistance of the metal surface.[22] Hydrogenating all the carbon atoms leads to the formation of cyclohexanol, which can readily desorb from the surface since all carbon atoms are already saturated. The shortest distance of cyclohexanol is from the O atom to the surface Pt atom at a distance of 2.67 Å (Figure 5A). This result also predicts that the cyclohexanone in low temperature hydrogenation of phenol on the Pt catalyst should be a minor product. This prediction is consistent with many experimental observations that cyclohexanol is the major product while cyclohexanone only accounts for a small fraction of the product, resulting in a high selectivity toward cyclohexanol for low temperature hydrogenation on the supported Pt catalysts.[15,17] However, the dominant reaction route may vary depending on different reaction conditions,

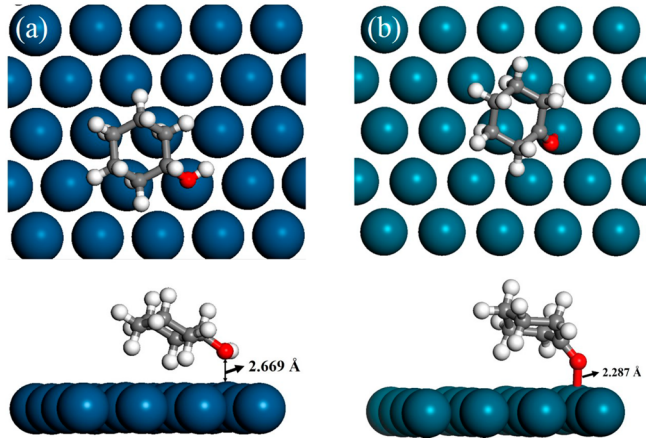

Figure 5. Top view (upper) and side view (lower) of (a) cyclohexanol on Pt (111), (b) cyclohexanone on Pd (111). The Pt and Pd atoms are in dark blue and light blue, respectively; the O, H, and C atoms are in red, white, and gray, respectively.

such as hydrogen partial pressure and temperature. For example, at relatively high temperatures, the formation of cyclohexanone became significant,[41] which could be interpreted as the high reaction temperature overcoming the difference between activation barriers and making the tautomerization pathway accessible, resulting in the formation of cyclohexanone.

As shown in the previous section, dissociatively adsorbed phenol (i.e., coadsorbed phenoxy and H adatom) is both thermodynamically and kinetically favored on the Pd(111) surface. Therefore, it is reasonable to assume that the hydrogenation starts with adding the hydrogen atom to the carbon atoms of the phenyl ring in turn. The intermediate formed by adding a hydrogen atom to C_1 has the highest adsorption energy (0.27 eV). This value is significantly higher than that of the intermediate formed from adding one hydrogen atom to C_1 of phenol on Pt(111) surface. Thus, hydrogenating C_1 is thermodynamically less favorable than starting hydrogenation from a different carbon atom. Note that the intermediates formed from adding a hydrogen atom to the ortho- (C_2 and C_6) and para- (C_4) positions have a similar energy between −0.31 eV to −0.37 eV, whereas the intermediates formed from hydrogenation at meta- (C_3 and C_5) positions have lower adsorption energies (−0.50 eV and −0.51 eV, respectively) and are significantly more stable.

Even though phenoxy is an important species on Pd(111), the hydrogenation of phenoxy may kinetically compete with the direct hydrogenation of the adsorbed phenol. To evaluate the relative contribution of adsorbed phenol and phenoxy to the hydrogenation product, the activation barriers of adding the first hydrogen to the C_6 of the phenyl ring of adsorbed phenol and phenoxy (Scheme 1) were calculated and compared in Figure 4b. It is evident that the barrier for phenol hydrogenation (1.22 eV) is significantly higher than that of the combined process of phenol dissociation and phenoxy hydrogenation (0.85 eV), strongly indicating that hydrogenation through the phenoxy species is the kinetically preferred pathway on the Pd surface. Consecutively adding four hydrogen atoms to the phenyl ring results in surface adsorbed cyclohexanone (Scheme 1), which interacts with the Pd surface through the oxygen atom of the carbonyl group while all the carbon atoms become detached from the surface due to C saturation (Figure 5b). The Pd−O bond distance is

DOI: 10.1021/cs501805y
ACS Catal. 2015, 5, 2009−2016

Table 1. Pre-Exponential Factor (A), Activation Energy (E_a), and Reaction Rate Constant (k) at 473 K of the Initial Elementary Steps Involved Phenol Hydrogenation on the Pt and Pd Surface

	A (s^{-1})		E_a (eV)		k (s^{-1})	
reaction	Pt	Pd	Pt	Pd	Pt	Pd
$C_6H_5OH^* + * \rightarrow C_6H_5O^* + H^*$	2.61×10^{13}	7.43×10^{12}	0.48	0.20	2.09×10^{8}	5.29×10^{10}
$C_6H_5O^* + H^* \rightarrow C_6H_5OH^* + *$	3.57×10^{13}	2.74×10^{12}	0.36	0.28	4.79×10^{9}	2.74×10^{9}
$C_6H_5OH^* + H^* \rightarrow C_6H_6OH^* + *$	8.17×10^{12}	6.02×10^{12}	0.94	1.23	8.72×10^{2}	5.30×10^{-1}
$C_6H_5O^* + H^* \rightarrow C_6H_6O^* + *$	1.15×10^{13}	1.98×10^{13}	0.96	0.67	6.18×10^{2}	1.44×10^{6}

2.29 Å, with an adsorption energy of −0.26 eV. If the adsorbed cyclohexanone was further hydrogenated, hydrogen would be added to the C_1 before O. The calculated barrier for adding hydrogen to C_1 of cyclohexanone (0.56 eV) is two times higher than the energy for cyclohexanone desorption (0.26 eV). Consequently, desorption of cyclohexanone is preferred over further hydrogenation of cyclohexanone on Pd at low temperatures (Scheme 1). Even though including van der Waals interactions increased the binding of cyclohexanone on the surface, making further hydrogenation possible, desorption may still be favorable because it is an entropy driven process.[42] In fact, the estimated entropy increase can overcome the effect of including van der Waals interactions for cyclohexanone by approximating adsorption as condensation. Consequently, desorption of cyclohexanone is expected to be more favorable than further hydrogenation.

The results from the present study predict that cyclohexanone is the major product for low temperature hydrogenation of phenol over supported Pd catalysts. Again, the prediction is consistent with the experimental results that Pd is the most selective catalyst for cyclohexanone production from phenol hydrogenation.[15] It should be noted that the increased formation of the phenoxy species on the surface is key to a high selectivity of cyclohexanone on the Pd-based catalysts. Therefore, one may expect that adding promoters that stabilize the surface phenoxy species and prevent its recombination with H adatoms will further improve the selectivity toward cyclohexanone. Indeed, Liu et al.[25] showed that adding Lewis acids to the supported Pd catalysts enhanced the stability of surface phenoxy, and thus, it significantly improves the selectivity to cyclohexanone for low-temperature hydrogenation of phenol.

We note that the energy difference for cyclohexanone desorption and further hydrogenation to cyclohexanol is only 0.3 eV, which indicates that increased reaction temperature would overcome the difference and make the hydrogenation channel accessible. A recent experimental study of hydrodeoxygenation of phenolics at relatively higher temperatures showed a significant amount of cyclohexanols although cyclohexanones were still the major intermediates,[17] in agreement of the present results.

We summarized the major reaction pathways for low temperature hydrogenation of phenol on Pt(111) and Pd(111) surfaces in Scheme 1. The very different selectivity of Pt and Pd for phenol hydrogenation originates from the very different relative stability of phenol and phenoxy species on the two surfaces. The difference in stability determines which species is abundant on the surface and accessible for hydrogenation. The formation of phenoxy species is both thermodynamically and kinetically favorable on Pd but unfavorable on Pt. On the Pt surface, the adsorbed phenol is the major surface species that is hydrogenated all the way to cyclohexanol, as the tautomerization of cyclohexenol to cyclohexanone is kinetically unfavorable. Therefore, cyclohexanol is the major product on Pt. In contrast, on the Pd surface, the initial species being hydrogenated is the adsorbed phenoxy, with cyclohexanone as the main product desorbing from the surface in low temperature hydrogenation. Consequently, cyclohexanone will be the dominant product on a Pd catalyst.

3.4. Microkinetics Analysis. Using the DFT calculated reaction energetics, we performed a microkinetics analysis based on the mean-field approximation. In addition to molecular adsorption of phenol and dissociative adsorption of hydrogen, we included four major elementary steps on the surfaces, i.e. (1) dissociation of adsorbed phenol to coadsorbed phenoxy and H adatom; (2) recombination of coadsorbed phenoxy and H adatom to adsorbed phenol; (3) the first hydrogenation step of adsorbed phenol; and (4) the first hydrogenation step of the surface phenoxy species. By assuming Langmuir adsorption behavior, we can estimate the adsorption constant based on the calculated adsorption energies and the estimated entropy changes from gas phase to the adsorbed species by approximating the change as condensation. Assuming that the harmonic transition state theory is applicable for the surface steps, the pre-exponential factor can be estimated from the normal-mode frequencies, υ_i, at the initial (IS) and transition (TS) states according to the following equation:

$$k = -\frac{k_B T}{h}\frac{q_{TS,vib}}{q_{IS,vib}} e^{-E_a/k_B T} \quad (2)$$

where k_B is the Boltzmann constant, T stands for the reaction temperature, h is the Planck's constant, and E_a denotes the zero-point energy corrected activation barrier from the DFT calculations. The vibrational partition functions of the transition and initial states, $q_{TS,vib}$ and $q_{IS,vib}$, can be evaluated using the calculated harmonic frequencies based on

$$q_{vib} = \prod_i \frac{1}{1 - e^{-h\nu_i/k_B T}} \quad (3)$$

where i runs to N-1 and N for the transition state and initial state, respectively.

Table 1 summaries the pre-exponential factors and activation barriers of the elementary steps on Pt and Pd obtained based on the DFT results. We also included the rate constants of these elementary steps on the Pt and Pd surfaces at 473 K. Clearly, dissociation of phenol on Pt is less favorable than the recombination reaction, whereas the order is reversed on Pd. Furthermore, the hydrogenation rate constants of adsorbed phenol and phenoxy on Pt are comparable while the hydrogenation rate constant of the surface phenoxy species on Pd is 7 orders of magnitude greater than that of surface phenol. These results indicate that although the surface phenoxy species can be formed on Pt, it is more likely to

DOI: 10.1021/cs501805y
ACS Catal. 2015, 5, 2009−2016

recombine with the surface H adatom to form adsorbed phenol before it is hydrogenated. In contrast, the surface phenoxy species can be more readily hydrogenated than recombine with the surface H adatoms on Pd.

On the basis of the kinetics data of the elementary steps listed in Table 1, we can determine the coverage ratio of phenol*/phenoxy* at 473 K and 1 bar of H_2. At steady state, the major surface species are phenol, phenoxy, and H, and the surface coverages of the intermediates formed from further hydrogenation can be assumed low and remain constant. The adsorption of phenol and the dissociative adsorption of H_2 can be treated as in quasi-equilibrium. To simplify the solution of the rate equations (see details in the Supporting Information), we also assumed that phenol, phenoxy, and H compete for the same surface sites. Under this approximation, the adsorption and rate equations are solvable analytically. Although this treatment is an approximation, the relative trends of the resultant phenol*/phenoxy* coverage ratio ($\theta_{phenol}/\theta_{phenoxy}$) and hydrogenation rate on Pt and Pd should be valid as it treated both surfaces equally. The surface coverage ratio of phenol*/phenoxy* is as high as 1.64×10^4 on Pt, whereas it is only 8.22 on Pd at 473 K and 1 bar H_2 (Table S1). This result indicates that phenol is the predominant species on Pt. Even on Pd, adsorbed phenol is still the majority species. On the other hand, the rate ratio of the first hydrogenation step on Pt and Pd for phenol and phenoxy are very different. At 473 K and 1 bar H_2, the rate ratio is 4.59×10^4 and 3.28×10^{-5} on Pt and Pd, respectively (Table S2), indicating that hydrogenation of the adsorbed phenol is dominant on Pt. In contrast, although adsorbed phenol is still the majority species, phenoxy will be hydrogenated once it is formed on Pd, making the hydrogenation of phenoxy and its subsequent steps as the leading pathway. This analysis provides further support to our hypothesis in section 3.2 that surface phenol is the dominant species on Pt and its direct hydrogenation to cyclohexanol is the major reaction path. The high selectivity of Pd toward cyclohexanone can be attributed to facile hydrogenation of the phenoxy species on the surface. The reaction pathways on Pt and Pd are summarized in Scheme 1.

4. CONCLUSION

The adsorption of phenol on the Pt(111) and Pd(111) surfaces leads to a similar most stable configuration, Bri 30, in which the phenyl ring is almost in parallel with the surface, and the hydroxyl group tilts away from the surface. In contrast, the most stable adsorption structures of phenoxy on Pt and Pd are very different; that is, both C_1 and O form bonds with the surface atoms on Pd whereas they tilt away from the surface on Pt. Calculated energetics and activation barriers indicate that phenol dissociation is both thermodynamically and kinetically unfavorable on Pt while favorable on Pd. Consequently, the adsorbed phenol would be the major species being hydrogenated on Pt, although phenoxy is likely to be the major species being hydrogenated on Pd. On Pt, the activation barrier for adding the first hydrogen atom to the adsorbed phenol is 0.49 eV lower than that for phenol dissociation to phenoxy followed by adding the first hydrogen atom to its phenyl ring, leading to direct hydrogenation of the surface adsorbed phenol to cyclohexanol as the major reaction pathway. In contrast, the activation barrier for the latter process is 0.37 eV lower than that for the former on Pd, resulting in hydrogenation of adsorbed phenoxy to cyclohexanone as the major reaction path. Microkinetics analysis provides further evidence to support the conclusion based on the DFT energetics. The present study showed that the relative stability of phenol and phenoxy depends critically on the nature of the catalysts, which will in turn determine the selectivity of hydrogenation and hydrodeoxygenation of phenol and phenolic compounds.

■ ASSOCIATED CONTENT

Supporting Information

The following file is available free of charge on the ACS Publications website at DOI: 10.1021/cs501805y.

Relaxed metastable adsorption structures of phenol on Pt(111) and Pd(111), the corresponding adsorption energies, surface coverages of phenol and phenoxy on Pt and Pd, and information about the relaxed atom coordinates of calculations (PDF)

■ AUTHOR INFORMATION

Corresponding Authors

*E-mail: xinlizhu@tju.edu.cn. Tel.:86-22-27890859 (X.Z.).
*E-mail: qge@chem.siu.edu. Tel.:1-618-453-6406 (Q.G.).

Notes

The authors declare no competing financial interest.

■ ACKNOWLEDGMENTS

The authors thank the support from the National Natural Sciences Foundation of China (Grant Nos. 21373148, 21206116, 21276191, and 21076152) and the Ministry of Education of China for Program of New Century Excellent Talents in University (NCET-12-0407). We also acknowledge the High Performance Computing Center of Tianjin University for providing services to our computing cluster and, in part, computing resources.

■ REFERENCES

(1) Mohan, D.; Pittman, C. U.; Steele, P. H. *Energy Fuels* **2006**, *20*, 848−889.
(2) Crossley, S.; Faria, J.; Shen, M.; Resasco, D. E. *Science* **2010**, *327*, 68−72.
(3) Hicks, J. C. *J. Phys. Chem. Lett.* **2011**, 2280−2287.
(4) Huber, G. W.; Iborra, S.; Corma, A. *Chem. Rev.* **2006**, *106*, 4044−4098.
(5) Zakzeski, J.; Bruijnincx, P. C.; Jongerius, A. L.; Weckhuysen, B. M. *Chem. Rev.* **2010**, *110*, 3552−99.
(6) Zhu, X. L.; Lobban, L. L.; Mallinson, R. G.; Resasco, D. E. *J. Catal.* **2011**, *281*, 21−29.
(7) Zhu, X. L.; Nie, L.; Lobban, L. L.; Mallinson, R. G.; Resasco, D. E. *Energy Fuels* **2014**, *28*, 4104−4111.
(8) Wang, H.; Male, J.; Wang, Y. *ACS Catal.* **2013**, *3*, 1047−1070.
(9) Hong, D. Y.; Miller, S. J.; Agrawal, P. K.; Jones, C. W. *Chem. Commun. (Cambridge, U. K.)* **2010**, *46*, 1038−40.
(10) Zhao, C.; Kou, Y.; Lemonidou, A. A.; Li, X.; Lercher, J. A. *Angew. Chem., Int. Ed.* **2009**, *48*, 3987−90.
(11) Massoth, F. E.; Politzer, P.; Concha, M. C.; Murray, J. S.; Jakowski, J.; Simons, J. *J. Phys. Chem. B* **2006**, *110*, 14283−91.
(12) Yoon, Y.; Rousseau, R.; Weber, R. S.; Mei, D.; Lercher, J. A. *J. Am. Chem. Soc.* **2014**, *136*, 10287−98.
(13) Sun, J. M.; Karim, A. M.; Zhang, H.; Kovarik, L.; Li, X. H. S.; Hensley, A. J.; McEwen, J. S.; Wang, Y. *J. Catal.* **2013**, *306*, 47−57.
(14) Shin, E. J.; Keane, M. A. *Ind. Eng. Chem. Res.* **2000**, *39*, 883−892.
(15) Talukdar, A. K.; Bhattacharyya, K. G. *Appl. Catal., A* **1993**, *96*, 229−239.
(16) Chen, C. W.; Huang, M. Y.; Jiang, Y. Y. *Macromol. Rapid Commun.* **1994**, *15*, 587−591.

DOI: 10.1021/cs501805y
ACS Catal. 2015, 5, 2009−2016

(17) Mortensen, P. M.; Grunwaldt, J. D.; Jensen, P. A.; Jensen, A. D. *ACS Catal.* **2013**, *3*, 1774−1785.
(18) Smith, H. A.; Stump, B. L. *J. Am. Chem. Soc.* **1961**, *83*, 2739−2743.
(19) Zhao, C.; Song, W.; Lercher, J. A. *ACS Catal.* **2012**, *2*, 2714−2723.
(20) Neri, G.; Visco, A. M.; Donato, A.; Milone, C.; Malentacchi, M.; Gubitosa, G. *Appl. Catal., A* **1994**, *110*, 49−59.
(21) Mahata, N.; Vishwanathan, V. *Catal. Today* **1999**, *49*, 65−69.
(22) Li, Y.; Xu, X.; Zhang, P. F.; Gong, Y. T.; Li, H. R.; Wang, Y. *Rsc Adv.* **2013**, *3*, 10973−10982.
(23) Wang, Y.; Yao, J.; Li, H.; Su, D.; Antonietti, M. *J. Am. Chem. Soc.* **2011**, *133*, 2362−5.
(24) Chen, Y. Z.; Liaw, C. W.; Lee, L. I. *Appl. Catal., A* **1999**, *177*, 1−8.
(25) Liu, H.; Jiang, T.; Han, B.; Liang, S.; Zhou, Y. *Science* **2009**, *326*, 1250−2.
(26) de Souza, P. M.; Nie, L.; Borges, L. E. P.; Noronha, F. B.; Resasco, D. E. *Catal. Lett.* **2014**, 1−7.
(27) Watanabe, S.; Arunajatesan, V. *Top. Catal.* **2010**, *53*, 1150−1152.
(28) Pérez, Y.; Fajardo, M.; Corma, A. *Catal. Commun.* **2011**, *12*, 1071−1074.
(29) Matos, J.; Corma, A. *Appl. Catal., A* **2011**, *404*, 103−112.
(30) Ihm, H.; White, J. M. *J. Phys. Chem. B* **2000**, *104*, 6202−6211.
(31) Honkela, M. L.; Bjork, J.; Persson, M. *Phys. Chem. Chem. Phys.* **2012**, *14*, 5849−54.
(32) Kresse, G.; Hafner, J. *Phys. Rev. B Condens Matter* **1993**, *47*, 558−561.
(33) Kresse, G.; Furthmüller, J. *Comput. Mater. Sci.* **1996**, *6*, 15−50.
(34) Blöch, P. E. *Phys. Rev. B: Condens. Matter Mater. Phys.* **1994**, *50*, 17953−17979.
(35) Kresse, G.; Joubert, D. *Phys. Rev. B: Condens. Matter Mater. Phys.* **1999**, *59*, 1758−1775.
(36) Perdew, J. P.; Burke, K.; Ernzerhof, M. *Phys. Rev. Lett.* **1996**, *77*, 3865−3868.
(37) Klimeš, J.; Bowler, D. R.; Michaelides, A. *Phys. Rev. B* **2011**, *83*, 195131.
(38) Ye, J.; Liu, C.-j.; Mei, D.; Ge, Q. *ACS Catal.* **2013**, *3*, 1296−1306.
(39) Orita, H.; Itoh, N. *Appl. Catal., A* **2004**, *258*, 17−23.
(40) Ye, J.; Liu, C-j..; Ge, Q. *Phys. Chem. Chem. Phys.* **2012**, *14*, 16660−7.
(41) Nie, L.; Resasco, D. E. *J. Catal.* **2014**, *317*, 22−29.
(42) Chiu, C.-c.; Genest, A.; Borgna, A.; Rösch, N. *ACS Catal.* **2014**, *4*, 4178−4188.

DOI: 10.1021/cs501805y
ACS Catal. 2015, 5, 2009−2016